

# 3-3 Generation of Telecom-band Quantum Entangled Photon Pairs and its Application to Quantum Key Distribution

TAKESUE Hiroki

Generation of quantum entangled photon pair in the 1.5- $\mu\text{m}$  telecom band is an important technology for realizing quantum communication systems over optical fiber networks. This paper reports generation of 1.5- $\mu\text{m}$  entangled photon pairs using spontaneous four-wave mixing in an optical fiber conducted by NTT Basic Research Laboratories. A new entanglement-based quantum key distribution scheme is also briefly described.

## **Keywords**

Quantum entanglement, Quantum key distribution

## **1 Introduction**

The technology for generating quantum entangled photon pairs is an important element in the construction of quantum information systems such as quantum key distribution and quantum computers. Previously, a quantum entangled pair generation source using spontaneous parametric down conversion (SPDC) was developed for the short wavelength band (0.7–0.8  $\mu\text{m}$ ) and has since been employed in various quantum information experiments[1][2]. However, to realize an advanced quantum info-communication system that operates on optical-fiber networks, it is essential to secure technology for generating quantum entangled photon pairs in the 1.5- $\mu\text{m}$  band, in which optical fiber loss is minimized.

This paper reports on the R&D efforts underway at the NTT Basic Research Laboratories to investigate technology for the generation of quantum entangled photon pairs in the telecom band and quantum key distribution

systems using this technology. Section 2 describes the technology for generating photon pairs with entangled states for time-bin and polarization using spontaneous four-wave mixing (SFWM) within optical fibers. In Section 3, a summary of a quantum key distribution protocol using higher-dimensional time-bin entangled photon pairs will be given as an example application of quantum entangled photon pairs. Finally, Section 4 will present the conclusions of the studies.

## **2 Generation of quantum entangled photon pairs using optical fibers**

### **2.1 Generation of quantum-correlated photon pairs by spontaneous four-wave mixing (SFWM) within optical fibers[3]**

SFWM is a process in which a signal/idler photon pair is created upon the annihilation of two pump photons due to three-dimensional non-linear optical effects[3][4]. If we assume

here that the two pump photons have the same angular frequency of  $\omega_p$ , and that the signal and idler photons have angular frequencies of  $\omega_s$  and  $\omega_i$ , respectively, then the following equation holds.

$$2\omega_p = \omega_s + \omega_i \quad (1)$$

The non-linear medium used here is a single-mode optical fiber, which is a fiber that normally displays small birefringence and has an optical axis that randomly changes direction in the longitudinal direction. When SFWM takes place in such a fiber, only signal/idler photon pairs with polarization identical to that of the pump photons are generated efficiently. For example, when pump photons with horizontal (H) polarization are used, a polarization-correlated photon pair state of  $|H\rangle_s|H\rangle_i$  is created by the SFWM process.

If the light intensity is sufficiently small, the phase-matching condition can be approximated by the expression below.

$$2k_p = k_s + k_i \quad (2)$$

Here,  $k_p$ ,  $k_s$ , and  $k_i$  are the wave numbers of the pump, signal, and idler photons, respectively. In the 1.5- $\mu\text{m}$  band, the above conditions may be attained using dispersion-shifted fiber (DSF) as the optical fiber and matching the wavelength of the pump light to the zero-dispersion wavelength of the DSF.

## 2.2 Generation of polarization-entangled photon pairs<sup>[5]</sup>

The loop fiber shown in Fig. 1 consisting of a DSF and polarization beam splitter (PBS) was used to generate a state of polarization entanglement using SFWM in the DSF. A pump light pulse having 45° linear polarization is input to this loop. The PBS separates the pump light into the H (horizontal) and V (vertical) polarization components. As the H and V components of the pump light propagate through the loop in the counterclockwise and clockwise directions, respectively, photon pair states of  $|H\rangle_s|H\rangle_i$  and  $|V\rangle_s|V\rangle_i$  are generated by the SFWM process. By controlling the pump light intensity appropriately, it is possi-

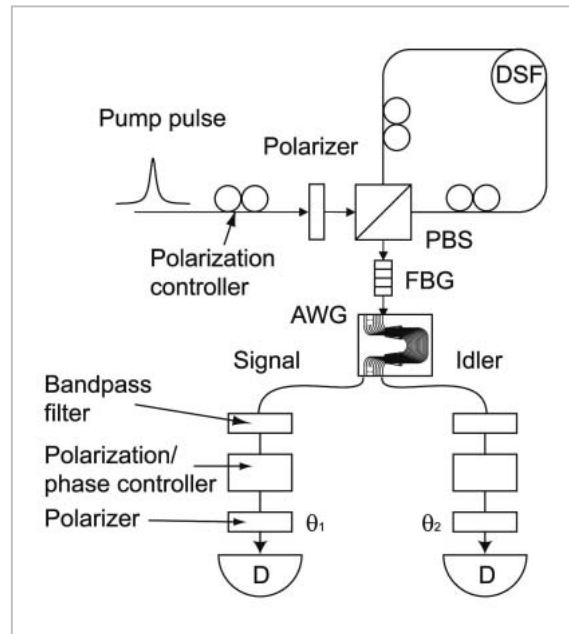


**Fig. 1** Generation of polarization-entangled photon pairs using fiber loop architecture (D: photon detector)

ble to minimize the probability of two pairs of photon twins being generated simultaneously. As a result, the state of superposition of  $|H\rangle_s|H\rangle_i$  and  $|V\rangle_s|V\rangle_i$ , or the polarization-entanglement state, may be obtained as an output of PBS. With the present architecture, both the H and V polarization components propagate through the same path, so the relative phase difference between the photon pair states  $|H\rangle_s|H\rangle_i$  and  $|V\rangle_s|V\rangle_i$  will remain constant at zero. Thus, we are able to create the stable state of polarization-entanglement represented by the following equation.

$$|\Phi\rangle = \frac{1}{\sqrt{2}}(|1\rangle_s|1\rangle_i + |2\rangle_s|2\rangle_i) \quad (3)$$

An experiment was conducted using the system shown in Fig. 1. A pump pulse with width of 20 ps, repetition of 100 MHz, and a central wavelength of 1551 nm was adjusted to have a 45° linear polarization and input to a fiber loop. The loop consisted of a PBS, a 2.5 km DSF with zero dispersion wavelength of 1551 nm, and two polarization controllers. After the light beam is input to the fiber Bragg grating (FBG) to remove the pump photons, it is then input to the arrayed waveguide grating (AWG) to separate the signal and idler pho-

tons. The central wavelengths of the signal and idler photons are 1552.7 and 1549.4 nm, respectively. Next, the signal and idler photons are further passed through a band-pass filter and then input to the polarization controller to correct any variations in polarity they may have experienced after the signal/idler photon separation process. They are then input to a rotating polarizer. After passing through the polarizer, the photons are received by photon detectors using InGaAs APD. Simultaneous counting of the signal and idler photons takes place by inputting the photon detection signals from the two detectors into a time interval analyzer. The quantum efficiency of both photon detectors was 10 %.

Figure 2 shows the resultant coincidence counting rate  $C(\theta_1, \theta_2)$  for a case in which the angle of rotation of the idler photon polarizer  $\theta_2$  is fixed at  $0^\circ$  and  $45^\circ$  while the angle of rotation of the signal photon polarizer  $\theta_1$  is changed. However, here, the effect of an accidental coincidence counting rate caused by noise photons resulting from spontaneous Raman scattering[3] within the optical fiber has been removed. It can be seen from the figure that a fairly good two-photon interference pattern with visibility exceeding 90 % was observed. Note that the visibility for the case in which the effects of an accidental coincidence counting rate is included was approximately 77 %.

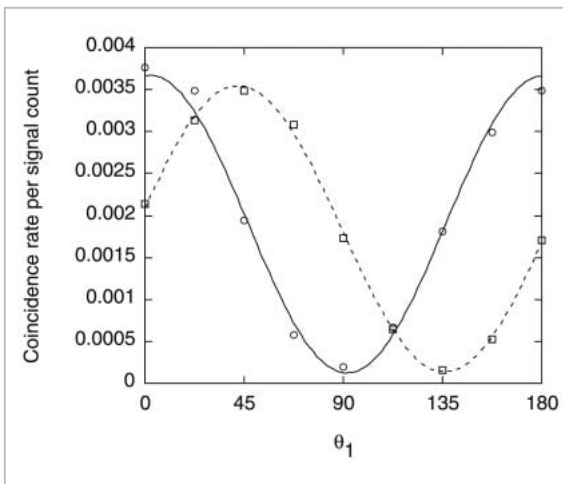


**Fig.2** Results of measurement of two-photon interference patterns (polarization entanglement)

Next, an experiment was carried out to test Bell's inequality based on the Clauser, Horne, Shimony, and Holt (CHSH) inequality. Five runs were performed to measure the  $S$  value, and as a result, we obtained

$$S = 2.65 \pm 0.09.$$

In other words, we were able to observe the violation of the CHSH inequality at a magnitude seven times larger than the standard deviation.

### 2.3 Generation of time-bin-entangled photon pairs

Quantum entanglement based on the polarized qubit, as described in the previous section, can be handled relatively easily in experiments in free space, and so this method has often been used in experiments in the short wavelength band. However, it is extremely difficult to control the polarization of photons inside an optical fiber. Furthermore, the dispersion of the polarization mode that occurs after fiber transmission over long distances causes deterioration in polarized qubit coherence. In contrast, the state of superposition of photons having different temporal locations offers characteristics rendering such photons favorable for use as qubits in optical-fiber transmissions. Thus, we have decided to use SFWM in optical fiber to generate time-bin entangled photon pairs.

The experimental system is presented in Fig. 3. Continuous light having a wavelength of 1551 nm is modulated using an intensity modulator into two pump pulse trains each with a width of 1 ns and a pulse width of 90 ps. After the two pulse trains are amplified using an Erbium Doped Fiber Amplifier (EDFA), the spontaneous noise from the EDFA is suppressed by an optical filter and the pulse trains are input to a DSF having a zero-dispersion wavelength of 1551 nm. The SFWM process in the DSF generates the following state of time-bin entanglement.

$$|\Phi\rangle = \frac{1}{\sqrt{2}} (|1\rangle_s |1\rangle_i + |2\rangle_s |2\rangle_i) \quad (4)$$

Here,  $|k\rangle_x$  is the state at which a single

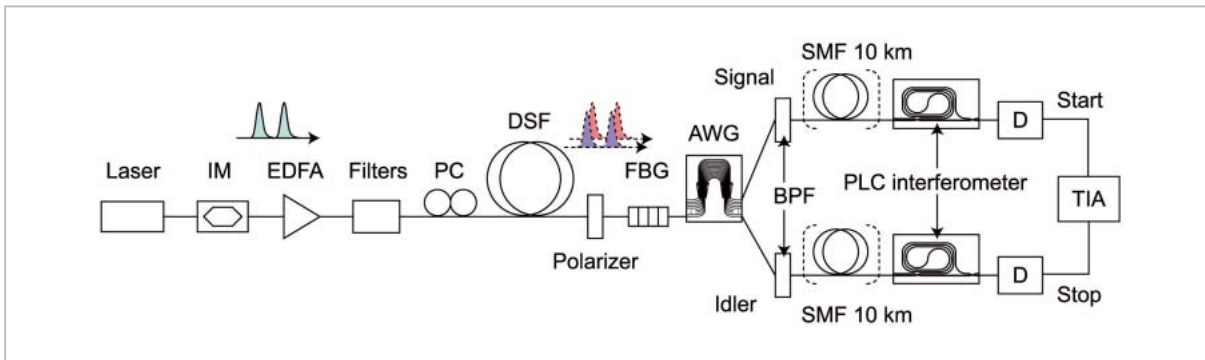


**Fig.3** Experimental system for time-bin-entangled photon pair generation (SMF: single-mode fiber; TIA: time-interval analyzer)

photon exists in mode  $x$  ( $s$ : signal;  $i$ : idler) at time slot  $k$ . After the pump light in the output from the DSF is suppressed by an optical filter system similar to that described in the previous section, the output photons are separated into signal and idler photons, and they are input to their respective paths, each having a planar lightwave circuit (PLC) delay interferometer with a difference in propagation delay of 1 ns. The signal and idler photons output from the interferometer are input to the photon detectors, and the counting rates and coincidence counting rates for both are measured. If we assume that  $\theta_s$  and  $\theta_i$  are the phase differences between the two paths through the interferometer for the signal and idler photons, then the state represented by Eq. (4) is converted into the equation below by the interferometer.

$$|\Phi\rangle \rightarrow |1\rangle_s |1\rangle_i + (\exp\{i(\theta_s + \theta_i)\} + 1) |2\rangle_s |2\rangle_i + \exp\{i(\theta_s + \theta_i)\} |3\rangle_s |3\rangle_i \quad (5)$$

Here, the common terms for amplitude have been omitted, and only the terms for coincidence counting are shown. The two-photon interference may be observed by measuring the coincidence counting rate in the second time slot.

The results of measurement of coincidence counting rates and idler counting rates in the case in which  $\theta_s$  is fixed and  $\theta_i$  is changed by changing the temperature of the idler interferometer is shown in Fig. 4. However, note that accidental coincidence counting rates are not

included. The results showed that a fairly good two-photon interference pattern having visibility of 99.3 % was obtained.

## 2.4 Suppression of noise photons by cooling of the optical fiber<sup>[7]</sup>

As stated above in Section 2, in the generation of quantum entanglement using SFWM in DSF, visibility of two-photon interference fringe is deteriorated by accidental coincidence counting caused by the noise photons created by spontaneous Raman scattering. The pump light for SFWM also acts as a pump for the Raman scattering process, and the pump light creates Stokes photons at longer wavelengths and anti-Stokes photons at shorter wavelengths. Therefore, in the coincidence counting of the photon pairs, accidental coincidence counting was induced by the Stokes/anti-Stokes photons having the same

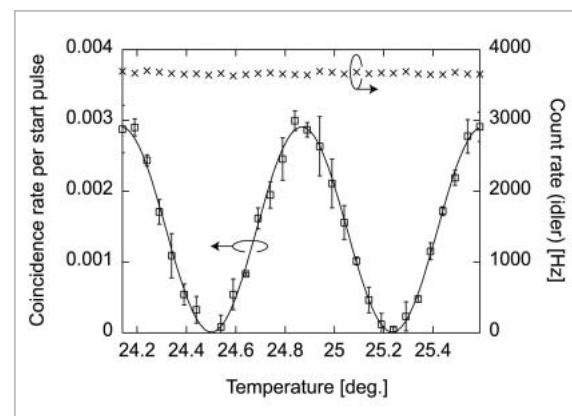


**Fig.4** Results of two-photon interference measurement (time-bin entanglement)

wavelength as the idler or signal photons generated by SFWM. Since accidental coincidence counting causes bit errors in quantum key distribution using quantum entanglement, as will be explained in Section 3, the suppression of noise photons is an important element of any actual application of this technology. Therefore, we have conducted an experiment for suppressing noise photon generation by suppressing lattice vibration through cooling of the DSF with liquid nitrogen.

Assuming spontaneous Raman scattering in an optical fiber with a loss factor of  $\alpha$ , the number of Stokes and anti-Stokes photons in a state of thermal equilibrium at temperature  $T$  [K] may be expressed as follows.

$$n_s(T) = \frac{gL e^{-\alpha L}}{1 - \exp\left(-\frac{h\nu}{k_B T}\right)} \quad (6)$$

$$n_{as}(T) = \frac{gL e^{-\alpha L}}{\exp\left(\frac{h\nu}{k_B T}\right) - 1}$$

Here,  $h$ ,  $k_B$ ,  $\nu$ ,  $L$ , and  $g$  are Planck's constant, Boltzmann's constant, the frequency of lattice vibration, fiber length, and gain, respectively. When  $\nu = 400$  GHz, the ratios of photon numbers at liquid nitrogen (77 K) and room (293 K) temperatures for Stokes and anti-Stokes photons at the same pump light intensity are calculated as  $n_s(77)/n_s(293) = 0.29$  and  $n_{as}(77)/n_{as}(293) = 0.24$ , respectively. It can be seen that by cooling the DSF with liquid nitrogen, it is possible to suppress the generation of noise photons to approximately one-fourth the degree otherwise observed.

An experiment was performed to confirm the above results. A pump pulse having a width of 100 ps and repetition of 100 MHz was input to a 500-m DSF cooled by liquid nitrogen, and the temporal correlation of the generated quantum-correlated photon pairs was measured. The ratio ( $C$ ) of coincidence count and accidental coincidence count was used as the index for temporal correlation. In other words,  $C > 1$  indicates the existence of a temporal correlation, and higher  $C$  values indicate a larger correlation. Figure 5 plots the measured  $C$  values as a function of the mean

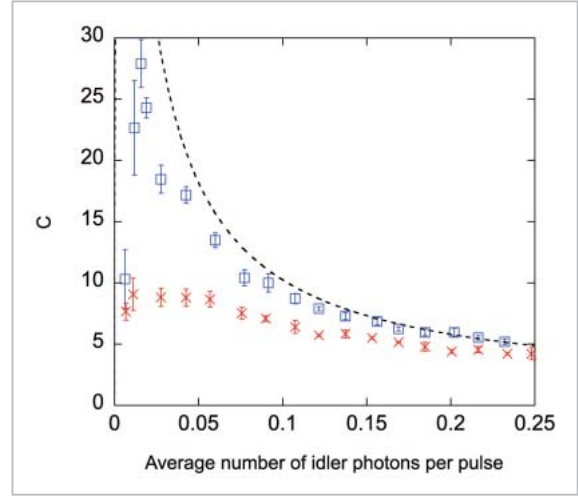


**Fig.5** Dependency of  $C$  values on idler photon number per pulse

idler photon number generated per pump pulse. At room temperature, the maximum value of  $C$  was  $\sim 9$  and when cooled, the value increased to nearly 30. (The mean idler photon numbers were 0.01 and 0.02, respectively.) The dotted line in Fig. 5 represents the results of calculation assuming that no noise photons are present. In the region in which the mean idler photon number exceeds 0.15, the  $C$  values measured in the cooled condition almost coincide with the calculation results for the noiseless photon pairs. Based on the results of the present experiment, it can be estimated that the number of noise photons generated during cooling of DSF is 0.26 times (Stokes photon) and 0.24 times (anti-Stokes photon) the numbers that would otherwise obtain, respectively. These results coincide well with the results of the above calculation and show that the effect of noise photons can be dramatically reduced by cooling of the optical fiber.

Open squares and crosses denote conditions of cooling and room temperatures, respectively. The dotted line shows the values of  $C$  when no noise photons are present.

## 2.5 Advantages of quantum entangled photon pair generation using optical fibers

The advantage of quantum entangled photon pair generation using optical fibers is, in terms of implementation, its facility in produc-

ing highly efficient coupling with a transmission optical fiber. This approach also has additional advantages, as follows. In most existing reports on quantum entangled photon pair generation using non-linear crystals and waveguides, the photon pair generation rates per band were small, and so the band for photon pair generation had to be expanded to levels of several to several tens of nanometers. As a result, the pulse is broadened by the dispersion effect during optical-fiber transmission, which posed a problem in terms of long-distance transmission. In contrast, the quantum entangled photon pair generated using optical fibers features high photon pair generation efficiency per band, and so it is possible to limit the band for photon pair generation to 0.2 nm (25 GHz). This permits long-distance fiber transmission using standard single-mode fiber having large dispersion in the 1.5  $\mu$ m band [5] [6].

### 3 Quantum key distribution using continuous pulse, time-bin entangled photon pairs [8]

One example application of quantum entangled photon pair generation in the telecom bands as described in the above section is seen in quantum key distribution over an optical-fiber network. Using quantum entangled photon pairs instead of the attenuated coherent light used mainly in existing quantum key distribution experiments, it is possible to extend the distance of secure quantum key distribution [9]. NTT has proposed a method which combines the protocol proposed by Bennett et al. (BBM 92) [10] with higher-dimensional time-bin entangled photon

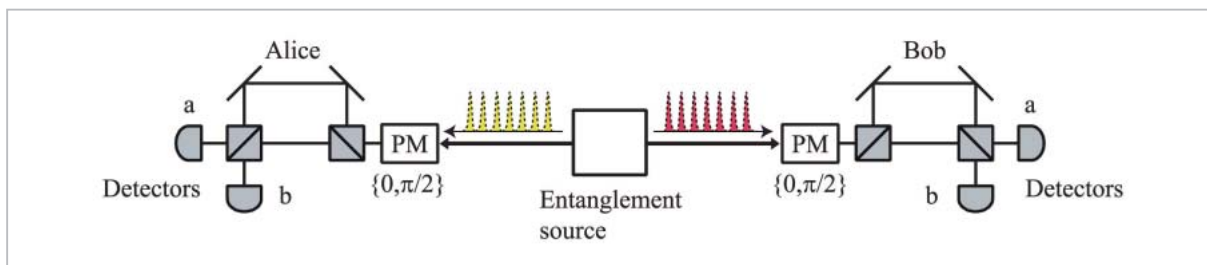
pairs to increase the key generation rate dramatically [8].

Figure 6 shows the architecture of the proposed method. From the light source, photon pairs with high-dimensional temporal locations expressed by the following equation are output.

$$|\Phi\rangle = \sum_k \sqrt{p} |k\rangle_s |k\rangle_i \quad (7)$$

Here,  $p$  is the probability of photon pair generation per unit time slot and is smaller than 1. As in the previous section,  $|k\rangle_x$  is the state at which a single photon exists in mode  $x$  ( $s$  : signal;  $i$  : idler) at time slot  $k$ . Time-bin entangled photon pairs with such high dimensions may be easily created by inputting, as pump light, continuous pulse trains having the same time interval as the delay times of the delay interferometers, following the procedures described in Section 2.3.

Of the output photon pair, one is sent to Alice and the other is sent to Bob. Both Alice and Bob apply random modulation  $\{0, \pi/2\}$  on the received photons using a phase modulator and then input the photons to a 1-bit delay interferometer. Both detect the photons output from the two output ports  $a$  and  $b$  of the interferometer using a photon detector, and the detected time and port are recorded. Alice and Bob disclose the data of the recorded time and the value of phase modulation at that time. In the case in which both Alice and Bob applied a phase modulation of 0, coincidence counting will always yield a positive correlation (in other words, detectors connected to the same port will click), while if phase modulation of  $\pi/2$  was applied by both, a negative correla-



**Fig.6** QKD system using high-dimensional time-bin entangled photon pairs

tion will be observed. On the other hand, when the two apply a different value for phase modulation, the observed results should display no correlation. Therefore, using coincidence counting only when the phase modulations of the two coincide, it is possible for Alice and Bob to secretly share identical bit trains. For example, Alice constantly allots bits of 0 and 1 to photon detection from ports a and b, respectively; Bob will do the same when he applies a phase modulation of 0, and will reverse the bits when he applies a phase modulation of  $\pi/2$ .

The present method utilizes the time domain more effectively than conventional quantum key distribution systems using quantum entanglement, and so it has the advantage of offering improved key generation rates.

## References

- 1 P. G. Kwiat, K. Mattle, H. Weinfurter, and A. Zeilinger, "New high-intensity source of polarization entangled photon pairs", *Phys. Rev. Lett.* 75, 4337, 1995.
- 2 P. G. Kwiat, E. Waks, A. G. White, I. Appelbaum, and P. H. Eberhard, "Ultrabright source of polarization-entangled photons", *Phys. Rev. A* 60, R773, 1999.
- 3 K. Inoue and K. Shimizu, "Generation of quantum correlated photon pairs in optical fiber: influence of spontaneous Raman scattering", *Jpn. J. Appl. Phys.* 43, 8048, 2004.
- 4 M. Fiorentino, P. L. Voss, J. E. Sharping, and P. Kumar, "All-fiber photon pair source for quantum communications", *IEEE Photon. Technol. Lett.* 14, 983, 2002.
- 5 H. Takesue and K. Inoue, "Generation of polarization entangled photon pairs and violation of Bell's inequality using spontaneous four-wave mixing in a fiber loop", *Phys. Rev. A* 70, 031802(R), 2004.
- 6 H. Takesue and K. Inoue, "Generation of 1.5-um band time-bin entanglement using spontaneous fiber four-wave mixing and planar lightwave circuit interferometers", *Phys. Rev. A* 72, 041804(R), 2005.
- 7 H. Takesue and K. Inoue, "1.5-um band quantum-correlated photon pair generation in dispersion-shifted fiber: suppression of noise photons by cooling fiber", *Opt. Express*, 13, 7832, 2005.
- 8 K. Inoue, "Quantum key distribution using a series of quantum correlated photon pairs", *Phys. Rev. A* 71, 032301, 2005.
- 9 E. Waks, A. Zeevi, and Y. Yamamoto, "Security of quantum key distribution with entangled photons against individual attacks", *Phys. Rev. A* 65, 052310, 2002.
- 10 C. H. Bennett, G. Brassard, and N. D. Mermin, "Quantum cryptography without Bell's theorem", *Phys. Rev. Lett.* 68, 557, 1992.

## 4 Conclusions

This paper described the generation of polarization-entangled and time-bin-entangled photon pairs in the 1.5- $\mu\text{m}$  band using optical fibers, and also reported on an experiment for suppressing spontaneous Raman scattering by cooling of the optical fiber. Furthermore, a new quantum key distribution system using high-dimensional time-bin-entangled photon pairs was proposed. We believe that the technology for generating quantum-entangled photon pairs described here will not only prove useful for quantum key distribution, but will also be an important elementary technology for advanced quantum info-communication systems such as quantum teleportation and quantum secret sharing.

---

**TAKESUE Hiroki, Ph.D.**  
*NTT Basic Research Laboratories, NTT  
Corporation*  
*Quantum Optics, Quantum Information*